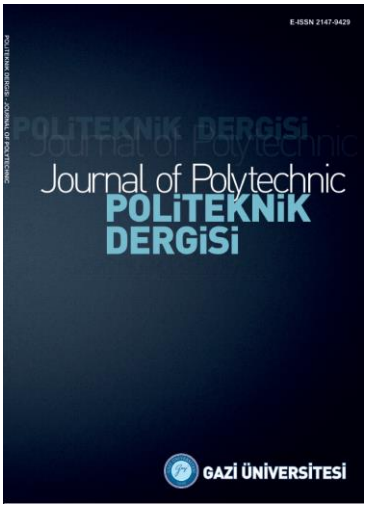

POLİTEKNİK DERGİSİ

JOURNAL of POLYTECHNIC

ISSN: 1302-0900 (PRINT), ISSN: 2147-9429 (ONLINE)
URL: http://dergipark.org.tr/politeknik

Simulation of PM10 and NOx pollutants at a coal-fired thermal power plant site using the gaussian plume model in freemat

Freemat'ta gauss tüy modeli kullanılarak kömür termik santrali sahasında PM10 ve NOx kirleticilerinin simülasyonu

***Author(s)**: Yusof-den JAMASALI[1], Şeref TURHAN[2], Aybaba HANÇERLİOĞULLARI[3], Aslı Kurnaz[4]*

ORCID[1]: 0000-0001-5259-9789

ORCID[2]: 0000-0005-5303-3680

ORCID[3]: 0000-0001-7008-480X

ORCID[4]: 0000-0002-7910-3461

To cite to this article: Jamasali Y., Turhan Ş., Hançerlioğulları A. and Kurnaz A., "Simulation of PM_{10} and NO_x Pollutants at a Coal-Fıred Thermal Power Plant Site Using The Gaussıan Plume Model in Freemat", ***Journal of Polytechnic***, *(*): *, (*).

To cite to this article: Jamasali Y., Turhan Ş., Hançerlioğulları A. ve Kurnaz A., "Simulation of PM_{10} and NO_x Pollutants at a Coal-Fıred Thermal Power Plant Site Using The Gaussıan Plume Model in Freemat", ***Politeknik Dergisi***, *(*): *, (*).

To link to this article: http://dergipark.org.tr/politeknik/archive

DOI: 10.2339/politeknik.1430492

Freemat'ta Gauss Tüy Modeli Kullanılarak Kömür Termik Santrali Sahasında PM10 Ve NOx Kirleticilerinin Simülasyonu

Simulation of PM10 and NO_x Pollutants at a Coal-Fired Thermal Power Plant Site Using the Gaussian Plume Model in Freemat

Highlights

- *Dispersion of PM_{10} and NO_x pollutants from Afşin-Elbistan A Thermal Power Plant has been simulated using the Gaussian Plume Model.*
- *The simulated ground concentrations were based on real data of the stacks, long-term winds, and appropriate stability classes.*
- *The ground concentration profiles of PM_{10} and NO_x pollutants show that in some regions it had exceeded the national standard limits.*

Graphical Abstract

The concept in numerical calculation and resulting ground concentration profile of dispersion of PM_{10} and NO_x pollutants from Afşin-Elbistan A Thermal Power Plant is shown in Figure below.

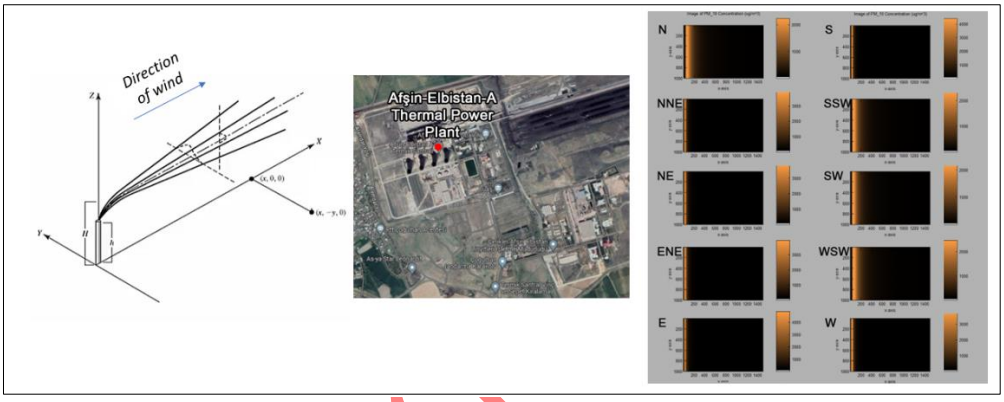

Figure. Orientation of Afşin-Elbistan A *Thermal Power Plant's stacks and simulation results.*

Aim

It is aimed to investigate ground concentrations of PM10 and NOx pollutants emitted by the stacks of Afşin-Elbistan A Thermal Power Plant.

Design & Methodology

Simulation of dispersion of PM10 and NOx pollutants in this study was carried out in Freemat software using the Gaussian Plume Model.

Originality

This study is original research due to the simulation technique and the model solely employed to investigate the ground concentrations of PM10 and NOx pollutants from Afşin-Elbistan A Thermal Power Plant, and never been done before.

Findings

The ground concentration profiles of PM_{10} and NO_x pollutants were obtained during winter and summer. The scenario with the highest maximum ground concentration of air pollutants is during summer with strong/moderate insolation wherein the ESE wind has 1.50 m/s speed. The ground concentrations of PM_{10} of 5380.77 $\mu g/m^3$ and NO_x of 767.09 $\mu g/m^3$ are both located at x =0.60 km. In contrast, the scenario with the least maximum ground concentration of air pollutants is during winter with slight insolation wherein the SW wind has 1.50 m/s speed. The ground concentration of PM_{10} of 1759.28 $\mu g/m^3$ and NO_x of 249.35 $\mu g/m^3$ are located at x =2.34 and 2.52 km, respectively.

Conclusion

It is concluded that scenarios of greatest maximum ground concentration values are less dispersed and are located near the stacks. Furthermore, regions where the ground concentrations of PM_{10} and NO_x exceed the Turkish government's national standard limit were also identified in all the scenarios.

Declaration of Ethical Standards

The authors of this article declare that the materials and methods used in this study do not require ethical committee permission and/or legal-special permission.

Simulation of PM10 and NO_X Pollutants at a Coal-Fired Thermal Power Plant Site Using the Gaussian Plume Model in Freemat

Araştırma Makalesi / Research Article

Yusof-den JAMASALI[1,2*], Şeref TURHAN[2], Aybaba HANÇERLİOĞULLARI[2], Aslı KURNAZ[2]

[1]Department of Physics, College of Natural Sciences and Mathematics, Mindanao State University-Main Campus, Marawi City

[2]Department of Physics, Kastamonu University, 37200 Kastamonu, Türkiye

(Geliş/Received : 02.02.2024 ; Kabul/Accepted : 25.03.2024 ; Erken Görünüm/Early View : 23.12.2024)

ABSTRACT

Air quality is important to both human health and the environment. But as modernization is progressing further, the problem of air quality has become more alarming. Using machines in factories, motor vehicles in transportation, and power plants in energy generation are major contributors to air pollution. Most power plants, including thermal power plants that burn coal to produce electricity, emit harmful pollutants into the atmosphere during energy generation. Turkish government encourages the exploitation of coal reserves for electricity generation to lessen the importation of energy sources. Hence, Türkiye relies mainly on coal in its energy production. As of this writing, there are 55 thermal power plants operating in Türkiye. These power plants had an installed capacity of 21 GW at the end of 2019. Among these are the Afşin-Elbistan Thermal Power Plants (AETPPs) located in Kahramanmaraş province. In this study, PM_{10} and NO_x pollutants at Afşin-Elbistan A Power Plant site located in Kahramanmaraş province of Türkiye were simulated using the Gaussian Plume Model in FreeMat software based on real data. The model input data included stack height, mass rate of emission of the pollutant, wind speed and direction, and atmospheric stability class. Dispersion profiles of PM_{10} and NO_x pollutants were generated and the locations of maximum values of concentrations were identified. Results show that during winter, the highest maximum concentration of PM_{10} and NO_x is 4865.79 $\mu g/m^3$ and 699.7 $\mu g/m^3$, respectively, with both located at x = 0.60 km in the scenario where 1.3-m/s wind is blowing from East. During summer, the highest maximum concentration of PM_{10} and NO_x is 5380.77 $\mu g/m^3$ and 767.87 $\mu g/m^3$, respectively, with both located at x = 0.60 km in the scenario where 1.5-m/s wind is blowing from East-South-East. Furthermore, regions where PM_{10} and NO_x concentrations exceed the national standard limit of 150 $\mu g/m^3$ and 100 $\mu g/m^3$, respectively, are always present and have been located in all the scenarios considered.

Keywords: FreeMat; NOx pollutants; PM10 pollutants; dispersion; Gaussian Plume Model, Afşin

Freemat'ta Gauss Tüy Modeli Kullanılarak Kömür Termik Santrali Sahasında PM10 ve NO_X Kirleticilerinin Simülasyonu

Araştırma Makalesi

ÖZ

Hava kalitesi hem insan sağlığı hem de çevre açısından önemlidir. Son yıllardaki nüfus, kentleşme, endüstri, ekonomi ve teknolojideki hızlı büyüme hava kalitesi sorununu daha da endişe verici hâle geldi. Bu hızlı büyüme elektrik enerjisine olan talebi de büyük oranda artırdı. Bu enerji talebini karşılamak için kurulan fosil yakıtlı termik santraller, çevre ve hava kirliliğinin ana kaynaklarını oluşturmaktadır. Hâli hazırda, Türkiye'de 53 termik santral faaliyet göstermektedir. Bu çalışmada köür yakıtlı Afşin-Elbistan A Elektrik Santrali sahasındaki PM_{10} ve NO_x (NO and NO_2) kirleticileri, meteorolojik esas alarak FreeMat yazılımındaki Gaussian Plume Modeli kullanılarak simüle edildi. Model girdi verileri, etkin baca yüksekliği, kirleticinin kütlesel salım oranı, rüzgâr hızı ve yönü ve atmosferik kararlılık sınıfı gibi verileri içermektedir. PM_{10} ve NO_x kirleticilerinin dağılım profilleri oluşturuldu ve azami derişim değerlerinin yerleri belirlendi. Kış ve yaz aylarında PM10 ve NO_x'in azami derişim değerleri, sırasıyla 4865 $\mu g/m^3$ ve 700 $\mu g/m^3$ ve 5381 $\mu g/m^3$ ve 768 $\mu g/m^3$ olarak bulundu. Simülasyon sonuçları PM_{10} ve NO_x derişimlerinin, ulusal standart sınır değerleri aştığın gösterdi.

Anahtar Kelimeler: FreeMat; NO_x kirletici; PM10 kirletici; dağılım; Gauss Tüy Modeli, Afşin

1. INTRODUCTION

Urbanization and continuous population growth have intertwined with the degradation of air quality in the atmosphere. Air pollution is not only caused by natural phenomena like volcanic eruptions but also by anthropogenic activities like power-producing stations, combustion engines, vehicles, and industrial machinery which are considered major sources of air pollution [1].

*Sorumlu Yazar (Corresponding Author)
e-mail: yusof-den.jamasali@msumain.edu.ph

Air quality is detrimental to both human health and the environment. It has been reported that long-term exposure is associated with pulmonary insufficiency, cardiovascular diseases, and cardiovascular mortality [2]. Short exposure to air pollution is related to several diseases like cough, chronic obstructive pulmonary disease, and even stroke or mortality from stroke [3]. Air pollution can also negatively affect the environment by polluting the precipitation, which then reaches the soil and hence, degrades the soil's quality [4].

Air pollutants are substances in the air with adequate amounts to cause harmful effects [5]. The major air pollutants are carbon monoxide (CO), nitrogen oxide (NO), nitrogen dioxide (NO_2), particulate matter (PM), lead, and tropospheric ozone.

Inhalable particulate matter (IP) are particles that enter the respiratory tract through the nose and mouth [6]. PM_{10} refers to IP <10 μm in diameter. And many toxic trace metals like lead (Pb) and mercury (Hg) could also be emitted into the atmosphere as PM [7].

On the other hand, Nitrogen oxides (NO_x) are comprised of NO and NO_2. Burning fossil fuels at high temperatures in the presence of nitrogen and oxygen produces NO, which rapidly converts to NO_2 in the atmosphere [8], [9]. Since molecular nitrogen is the main constituent of air, combustion of all fuels, even fuels with no nitrogen component, can yield NO_x. NO_x contributes to the formation of tropospheric ozone and nitrate aerosols, which are major air pollutants themselves.

Atmospheric emissions of NOx also contribute to the formation of the photochemical smog prevalent in many urban areas. Thus, they have a general detrimental effect on the respiratory health of humans and animals, as well as, on visibility [10]. Moreover, high levels of NO_x are also known to reduce crop yield [1].

To address this global issue, private agencies and governments have laid out ways to monitor air quality, proposed mechanisms, and legislated policies to curtail the emission of air pollutants. US Environmental Protection Agency (US EPA) developed the Air Quality Index (AQI) [11] to monitor air quality and to predict future values based on present measured values [12].

The AQI system has been successfully utilized to investigate air pollution in many countries such as China [13], India [14], [15], Malaysia [16] and Europe [17].

In Türkiye, the National AQI was launched in 2007 [18]. Furthermore, certain policy guidelines have been implemented for known point sources of air pollutants. Towards this end, for instance, the government in China urged the installation of air pollution control devices (APCDs), electrostatic precipitators (ESP), flue gas desulfurization (FGD) and selective catalytic reduction (SCR) in most coal-fired thermal power plants (TPP) in the recent years [19].

To monitor air quality, detectors are placed in several appropriate locations in a region. Practically, these detectors are not situated near one another to generate an inventory of air quality over the region. This is where modeling and its simulation of real data become useful. By simply knowing some information from installed detectors, modeling can determine the air quality in between. Hence, the profile of air quality across an entire region could be depicted.

One of the successful models most commonly used in simulating gas dispersion from point sources is the Gaussian Plume Model (GPM), developed by Pasquill [5]. Turbulent dispersion in the atmosphere can be described using both the Euler and Lagrange methods [20]. An example of commercial software that employs the Lagrangian Gaussian Plume Model is CALPUFF [21].

Among the primary sources of air pollutants is the combustion of coal, particularly in the production of electricity from TPP [22]. Meanwhile, Türkiye has huge domestic coal deposits [23]. Turkish government encourages the exploitation of these reserves for electricity generation to lessen the importation of energy sources [24].

Hence, Türkiye heavily depends on coal for its energy production. Consequently, extensive studies have been conducted to assess the cost and profit [25], and the advantages of implementing flue gas purification systems [26] in the utilization of coal as an energy source. Additionally, some studies have also examined the flexibility of coal-fired thermal power plants, particularly in acknowledgment of the increasing presence of renewable energy sources aimed at balancing the load in the power grid [27].

A s of this writing, 55 TPPs are operating in Türkiye [28]. These power plants had an installed capacity of 21 GW at the end of 2019. One of these is the Afşin-Elbistan-A Thermal Power Plants (AE-ATPP) located in Kahramanmaraş province, as shown in Figure 1. It was built from 1984 to 1987 and has been operating since then. It is designed for annual electricity production of 8,800,000,000 kWh. Currently, it has 4 units with a total power of 1360 MW and a gross generation of 4198 GWh of energy.

In this study, dispersion of PM_{10} and NO_x from the stacks of AE-ATPP has been simulated using GPM in the open-source software *FreeMat*. Data about air pollutants, stacks of the TPP, and available meteorological data at AE-ATPP were among the input parameters in the simulation.

2. MATERIAL AND METHOD

2.1. Gaussian Plume Model

The following are the assumptions in the GPM [5], [20]:

(1) The pollutant emissions are continuous;
(2) The pollutants are not reacting chemically in the atmosphere;

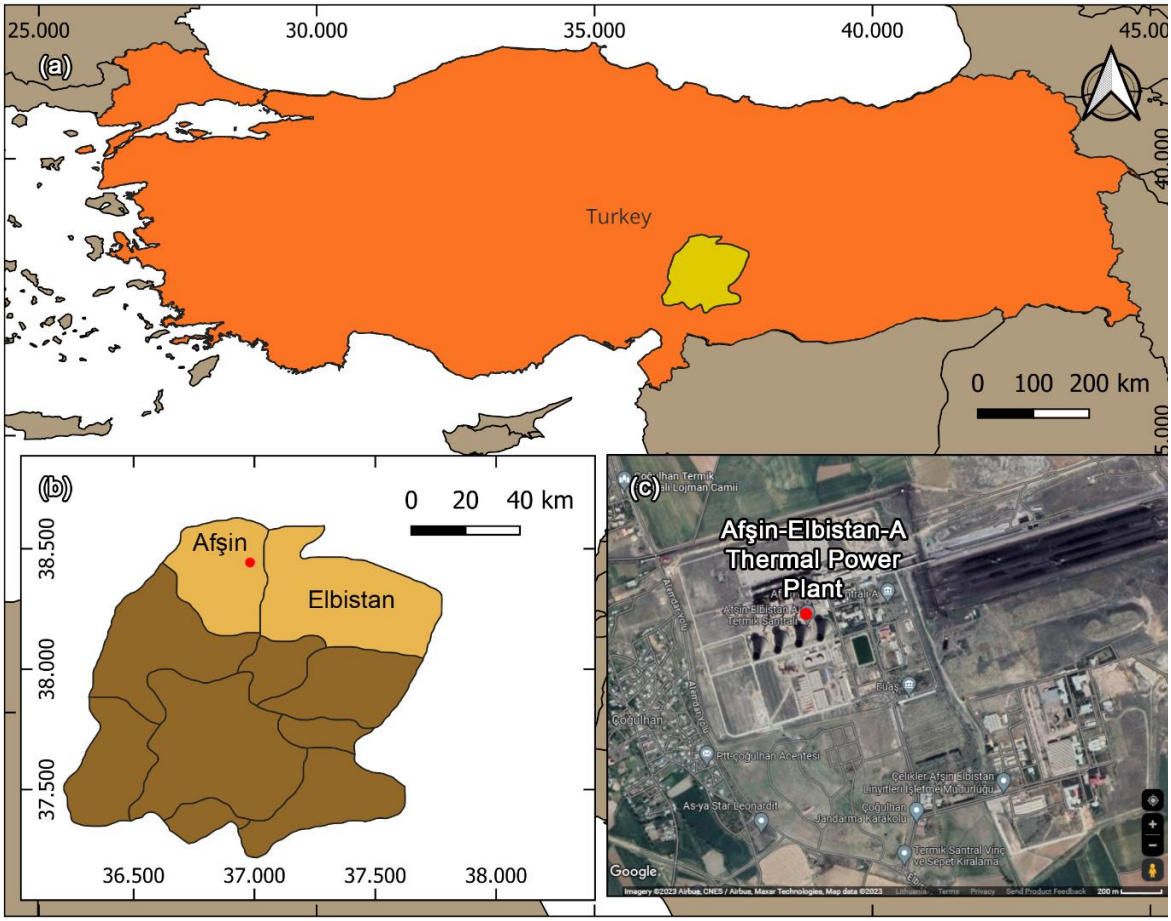

Figure 1. Geographical map of (a) Turkey (b) Kahramanmaraş Province and (c) Afşin-Elbistan-A Thermal Power Plant.

(3) At the wind direction the transport process is dominant to the turbulent dispersion;
(4) The aerosol diameter is smaller than 20 μm for their residence time in the atmosphere to be larger than the time intervals which are studied;
(5) The atmosphere is a stationary condition concerning the meteorological parameters for the time interval of transport from the pollution source to the receptors;
(6) Crosswinds are minimal/negligible;
(7) Terrain is flat near the source;
(8) Plumes from different sources do not interact, and
(9) Statistically normal distribution patterns are followed.

2.2. Main Parameters

The concentrations of pollutants occurring downwind are a function of effective stack height (H), mass rate of emission of the pollutant, wind speed and direction, and atmospheric stability. The basic equation of ground-level concentration of air pollutants in the GPM is given as follows [5], [20]:

$$C = \frac{E}{\pi s_y s_z u}\left[exp\left[-\frac{1}{2}\left(\frac{y}{s_y}\right)^2\right] exp\left[-\frac{1}{2}\left(\frac{H}{s_z}\right)^2\right]\right] \quad \text{Eq. 1}$$

where E is emission rate pollutant (g/sec), u is wind speed (m/sec), s_y and s_z are standard deviations, H is effective stack height and y is coordinate perpendicular to the wind's direction. The effective stack height H has the expression as follows [20], [29]:

$$H = h + \Delta H \quad \text{Eq. 2}$$

$$\Delta H = \frac{v_s d}{u}\left[1.5 + \left(2.68 \times 10^{-2}(P)\left(\frac{T_s - T_a}{T_s}\right) d\right)\right] \quad \text{Eq. 3}$$

where h is the physical height (m), v_s is the emission of speed from the main stack, d is stack diameter (m), u is wind speed (m/sec), P is pressure (kPa), T_s is stack temperature (K) and T_a is air temperature (K). In this study, there are four stacks emitting air pollutants. So, the

Table 1. Site-specific input parameters

Main Stack		**Bruden stack**	
Main stack height	145 m	Stack height	120 m
Main stack diameter	6.8 m	Stack diameter	3 m
Gas velocity	24 m/s	Gas velocity	15.8 m/s
Stack temperature	483 K	Stack temperature	378 K
Flow rates			
NO_x	686 kg/h	NO_x	98 kg/h
PM_{10}	3000 kg/h	PM_{10}	1000 kg/h

appropriate version of the equation of ground-level concentration of air pollutants in the GPM is given as follows:

$$C = \sum_{i=1}^{4} \frac{E_i}{\pi s_{yi} s_{zi} u} \left[exp\left[-\frac{1}{2}\left(\frac{y_i - y_{i0}}{s_{yi}} \right)^2 \right] exp\left[-\frac{1}{2}\left(\frac{H_i}{s_{zi}} \right)^2 \right] \right] \quad \text{Eq. 4}$$

where y_{i0} is the position of ith stack along the y-axis. The specific input parameters in the present study are listed in Tables 1 and 2.

2.3. Freemat algorithm

Since there are four stacks of AE-ATPP, all of these contribute to the ground concentration calculation. Stacks stand in a line with about 75 m distance apart. This line deviates by 14º from-West-to-East axis. In all the considered scenarios origin of the x-axis is always placed at the main stack and it is always oriented parallel to the direction of the wind.

Table 2. Long-term wind direction and average wind values at the Afşin Elbistan-A Thermal Power Plant and their stability classification during winter and summer

Wind Direction	Wind speed (m/s)	Insolation	
		Strong/ Moderate	Slight
N	2.8	B	C
NNE	1.9	A	B
NE	1.6	A	B
ENE	1.3	A	B
E	1.3	A	B
ESE	1.5	A	B
SE	2.2	B	C
SSE	1.7	A	B
S	1.9	A	B
SSW	2.7	B	C
SW	3.3	B	C
WSW	2.2	B	C
W	1.6	A	B
WNW	1.7	A	B
NW	3	B	C
NNW	2.7	B	C

3. RESULTS AND DISCUSSION

3.1. During Winter (January)

PM_{10} dispersion profiles during winter with strong/moderate and slight insolation are shown in Figure 2 and Figure 3, respectively. The maximum value of PM_{10} concentration, its location, and the region where the concentration exceeds the national standard limit of 150 µg/m^3 [30] are summarized in Table 3. During winter strong/moderate insolation the scenario with the highest maximum concentration is E where the value is 4865.79 µg/m^3 located at x = 0.60 km whereas the scenario with the least maximum value is NW with 2161.43 µg/m^3 at x = 1.30 km. On the other hand, during the same season but with slight insolation the scenario with the highest maximum concentration is still E where the value is 2576.86 µg/m^3 located at x = 1.74 km whereas the scenario with the least maximum value is SW with 1759.28 µg/m^3 at x = 2.34 km. That is, when the insolation is slight, the location of maximum concentrations is farther away from the stacks of the AE-ATPP. The farthest shift of maximum value is the scenario WSW from x = 1.34 km to x = 2.74 km while the least shifts are scenarios NNE from x = 0.64 km to 1.56 km and S from x = 0.62 km to x = 1.54 km.

NO_x dispersion profiles during winter with strong/moderate and slight insolation are shown in Figure 4 and Figure 5, respectively. The maximum value of NO_x concentration, its location, and the region where the concentration exceeds the national standard limit of 100 µg/m^3 [30] are summarized in Table 3(a,b). During winter strong/moderate insolation the scenario with the highest maximum concentration is E where the value is 699.7 µg/m^3 located at x = 0.6 km whereas the scenario with the least maximum value is NW with 310.31 µg/m^3 at x = 1.44 km. On the other hand, during the same season but with slight insolation the scenario with the highest maximum concentration is W where the value is 355.92 µg/m^3 located at x = 1.78 km whereas the scenario with the least maximum value is 249.35 µg/m^3 at x = 2.52 km. When the insolation shifts from strong/moderate to slight, the farthest shift of maximum value is the scenario WSW from x = 1.44 km to x = 3.02 km while the smallest shift is the scenarios NNE and S from x = 0.68 km to x = 1.72 km and from x = 0.64 km to x = 1.68 km, respectively.

3.2. During Summer (July)

PM_{10} Dispersion profiles during summer with strong/moderate and slight insolation are shown in Figure 6 and Figure 7, respectively. The maximum value of PM_{10} concentration, its location, and the region where the concentration exceeds the national standard limit of 150 µg/m^3 [30] are summarized in Table 4(a,b). During summer with strong/moderate insolation the scenario with the highest maximum concentration is ESE where the value is 5380.77 µg/m^3 located at x = 0.60 km whereas the NW scenario with the least maximum value is 2321.72 µg/m^3 at x = 1.26 km.

On the other hand, during the same season but with slight insolation the scenario with the highest maximum concentration is E where the value is 2899.71 µg/m^3 located at x = 1.62 km whereas the scenario with the least maximum value is SW with 1896.59 µg/m^3 at x = 2.22 km.

NO_x dispersion profiles during summer with strong/moderate and slight insolation are shown in Figure

8 and Figure 9, respectively. The maximum value of NO_x concentration, its location, and the region where the concentration exceeds the national standard limit of 100 µg/m^3 [30] are summarized in Table 4(a,b). During summer with strong/moderate insolation the scenario with the highest maximum concentration is ESE where the value is 767.87 µg/m^3 located at x = 0.60 km whereas the scenario with the least maximum value is NW with 332.08 µg/m^3 at x = 1.38 km. On the other hand, during the same season but with slight insolation the scenario with the highest maximum concentration is E where the value is 395.86 µg/m^3 located at x = 1.62 km whereas the scenario with the least maximum value is SW with 267.80 µg/m^3 at *x* = 2.42 km.

The findings of this study are in agreement with a study on the dispersion of air pollutants and heavy metal deposition emanating from AE-ATPP, employing the CALPUFF model over an extended geographical region [24].

It reported an alarming observation that the maximum 24-hour PM_{10} concentration recorded within the TPP's vicinity has exceeded the World Health Organization (WHO) guideline for PM_{10} by a factor of 7 [31].

Furthermore, the current study's outcomes exhibit congruence with prior research conducted on PM concentration surrounding the Manjung TPP in Malaysia [16]. It showed that seasonal variations in PM concentration demonstrated higher levels in July compared to March. Another study that is in the same agreement was on the measurement of the concentration of NO_x, SO_2, and several other air pollutants from TPPs of different technologies in Pakistan [10]. These studies suggest a discernible influence of meteorological parameters such as wind speed and temperature, the latter being closely associated with insolation levels. These underscores some correlations between climatic factors and airborne pollutant dispersion dynamics.

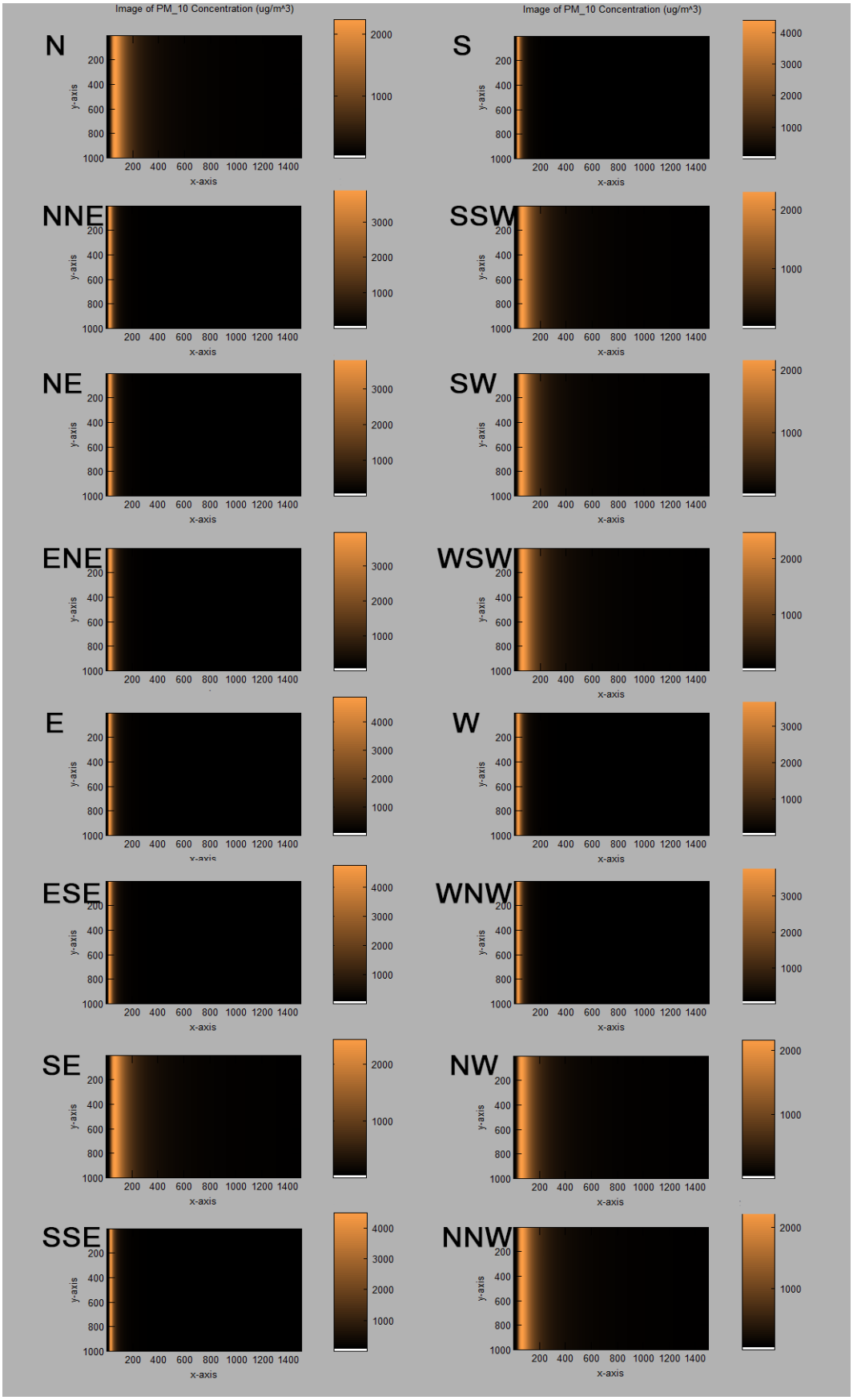

Figure 2. Dispersion profile of PM_{10} pollutants during winter with strong/moderate insolation

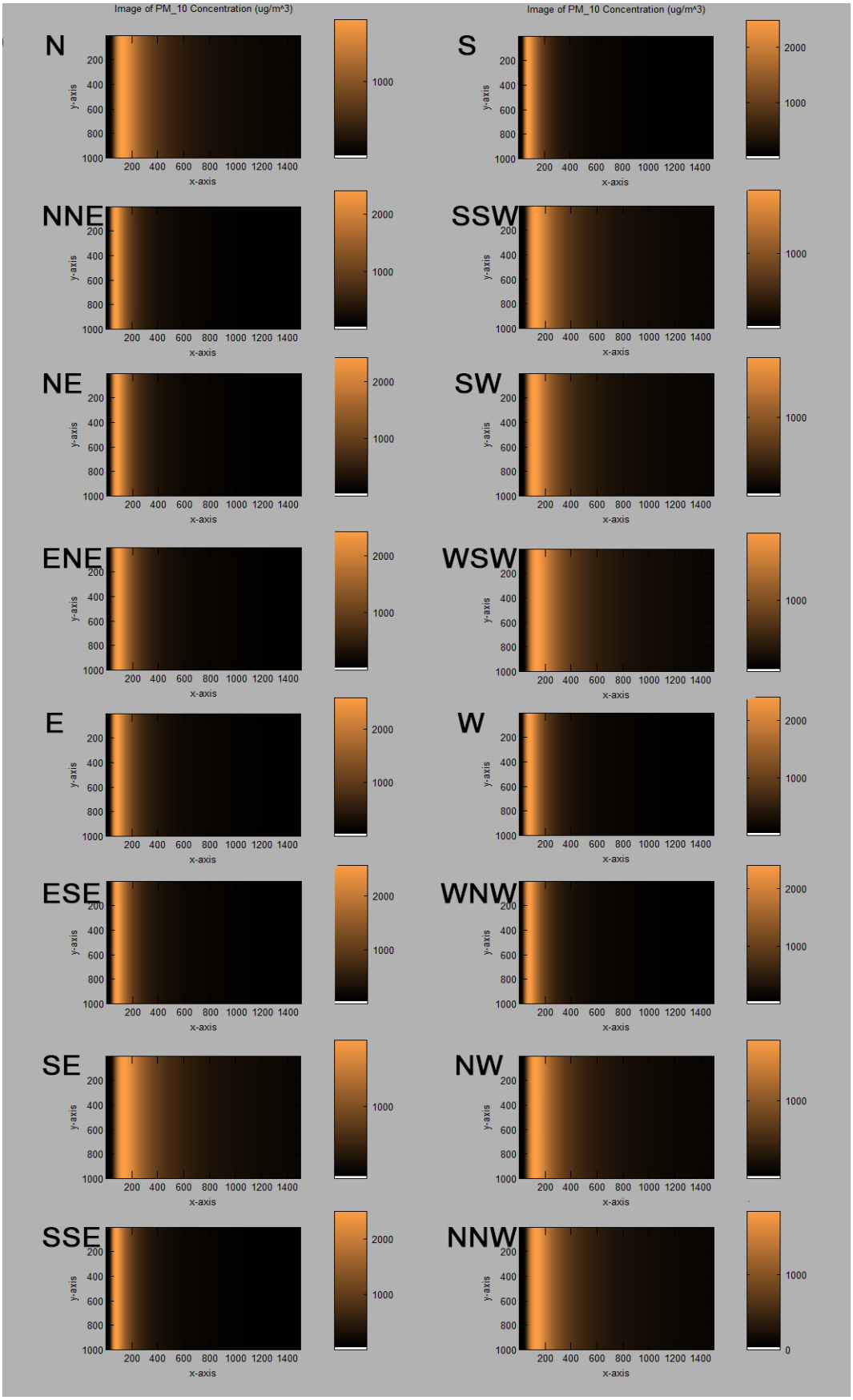

Figure 3. Dispersion profile of PM_{10} pollutants during winter with slight insolation

Table 3(a). Summary of dispersion profile of PM_{10} and NO_x pollutants at AE-ATPP during winter

Wind Direction	Strong/moderate insolation							
	PM_{10}				NO_x			
	Region Exceeding National Standard Limit (150 µg/m^3) x (km)		Maximum value (µg/m^3)	Location of maximum value x (km)	Region Exceeding National Standard Limit (100 µg/m^3) x (km)		Maximum value (µg/m^3)	Location of maximum value x (km)
	From	To			From	To		
N	0.5	8.44	2235.41	1.36	0.74	4.02	319.34	1.48
NNE	0.24	2.8	3893.78	0.64	0.32	1.7	578.01	0.68
NE	0.2	2.98	3883.32	0.66	0.3	1.8	582.51	0.72
ENE	0.2	3.2	3958.37	0.7	0.3	1.92	593.74	0.76
E	0.48	3.34	4865.79	0.6	0.54	2.02	699.7	0.6
ESE	0.45	3.16	4741.68	0.6	0.52	1.9	684.17	0.6
SE	0.66	9.55	2438.39	1.42	0.88	4.6	343.88	1.52
SSE	0.37	2.97	4484.68	0.66	0.45	1.79	646.42	0.68
S	0.39	2.87	4392.53	0.62	0.45	1.73	634.79	0.64
SSW	0.63	8.65	2325.41	1.3	0.83	4.15	330.79	1.38
SW	0.63	7.85	2190.22	1.18	0.81	3.75	314.18	1.24
WSW	0.7	9.6	2467.94	1.34	0.92	4.62	348.16	1.44
W	0.18	2.96	3800.22	0.66	0.28	1.78	574.85	0.72
WNW	0.22	2.9	3860.94	0.64	0.3	1.76	578.53	0.7
NW	0.44	8.12	2161.43	1.3	0.7	3.88	310.31	1.44
NNW	0.52	8.6	2268.12	1.38	0.76	4.1	323.34	1.5

Table 3(b). Summary of dispersion profile of PM_{10} and NO_x pollutants at AE-ATPP during winter

Wind Direction	Slight insolation							
	PM_{10}				**NO_x**			
	Region Exceeding National Standard Limit (150 µg/m^3) x (km)		Maximum value (µg/m^3)	Location of maximum value x (km)	Region Exceeding National Standard Limit (100 µg/m^3) x (km)		Maximum value (µg/m^3)	Location of maximum value x (km)
	From	To			From	To		
N	0.92	18.42	1809.94	2.6	1.42	7.8	255	2.86
NNE	0.52	10.18	2400.52	1.56	0.78	4.88	338.08	1.72
NE	0.52	11.08	2417.5	1.66	0.82	5.32	338.48	1.86
ENE	0.56	12.26	2417.58	1.82	0.88	5.88	335.53	2.08
E	0.86	12.42	2576.86	1.74	1.12	5.98	355	1.9
ESE	0.78	11.56	2567.18	1.64	1.04	5.56	355.92	1.78
SE	1.116	21.14	1919.32	2.82	1.62	8.98	266.89	3.1
SSE	0.67	10.81	2500.03	1.64	0.91	5.19	348.85	1.8
S	0.65	10.25	2477.27	1.54	0.89	4.93	347.31	1.68
SSW	1.05	18.85	1851.78	2.56	1.51	8.01	260.08	2.8
SW	1.03	16.89	1759.28	2.34	1.45	7.15	249.35	2.52
WSW	1.18	21.16	1932.75	2.74	1.66	9	268.67	3.02
W	0.5	11.06	2405.9	1.66	0.8	5.3	337.22	1.86
WNW	0.52	10.74	2410.89	1.62	0.8	5.16	338.37	1.82
NW	0.86	17.7	1768.16	2.52	1.36	7.48	250.11	2.78
NNW	0.99	18.83	1838.34	2.64	1.47	7.97	258.35	2.88

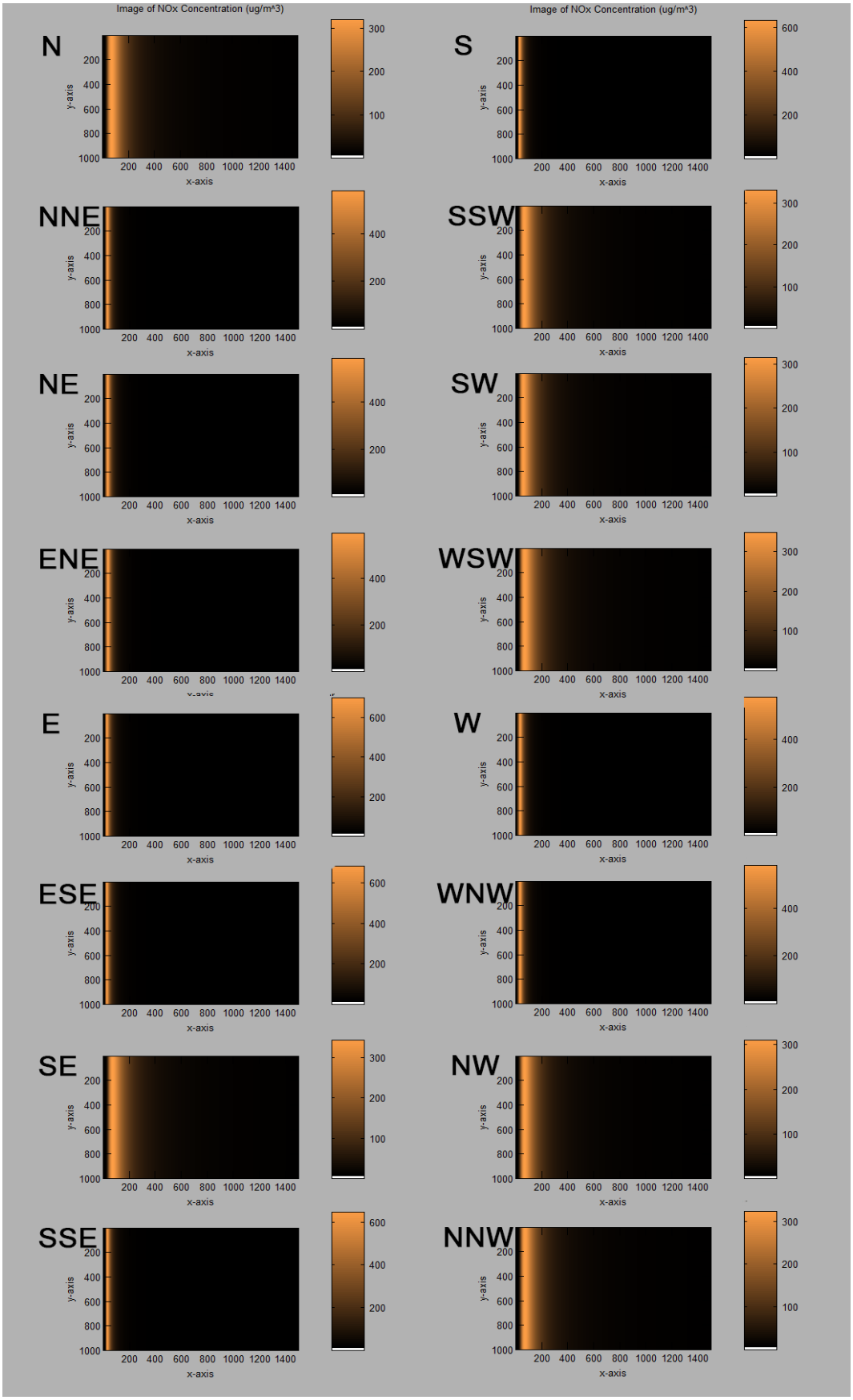

Figure 4. Dispersion profile of NO_x pollutants during winter with strong/moderate insolation

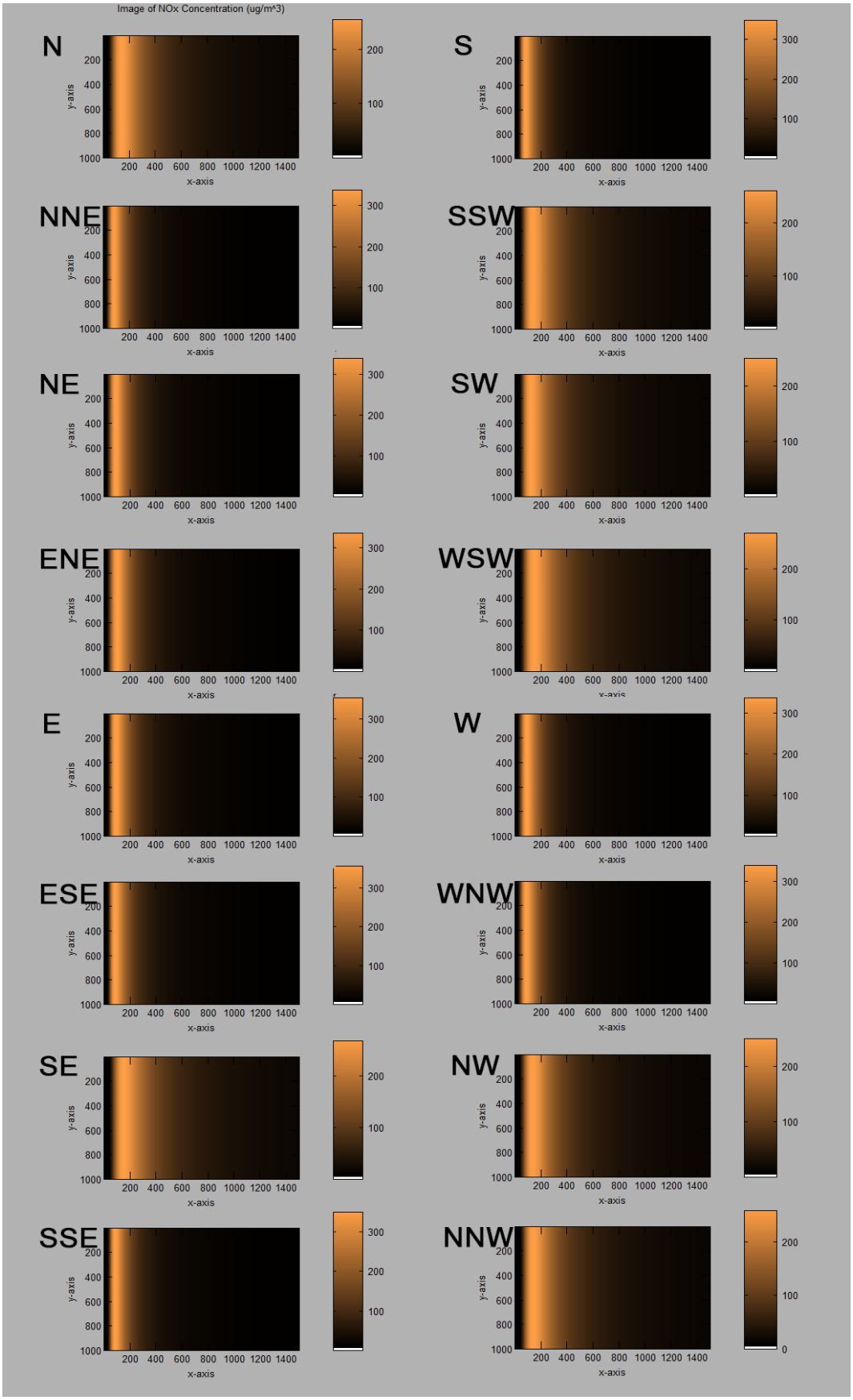

Figure 5. Dispersion profile of NO_x pollutants during winter with slight insolation

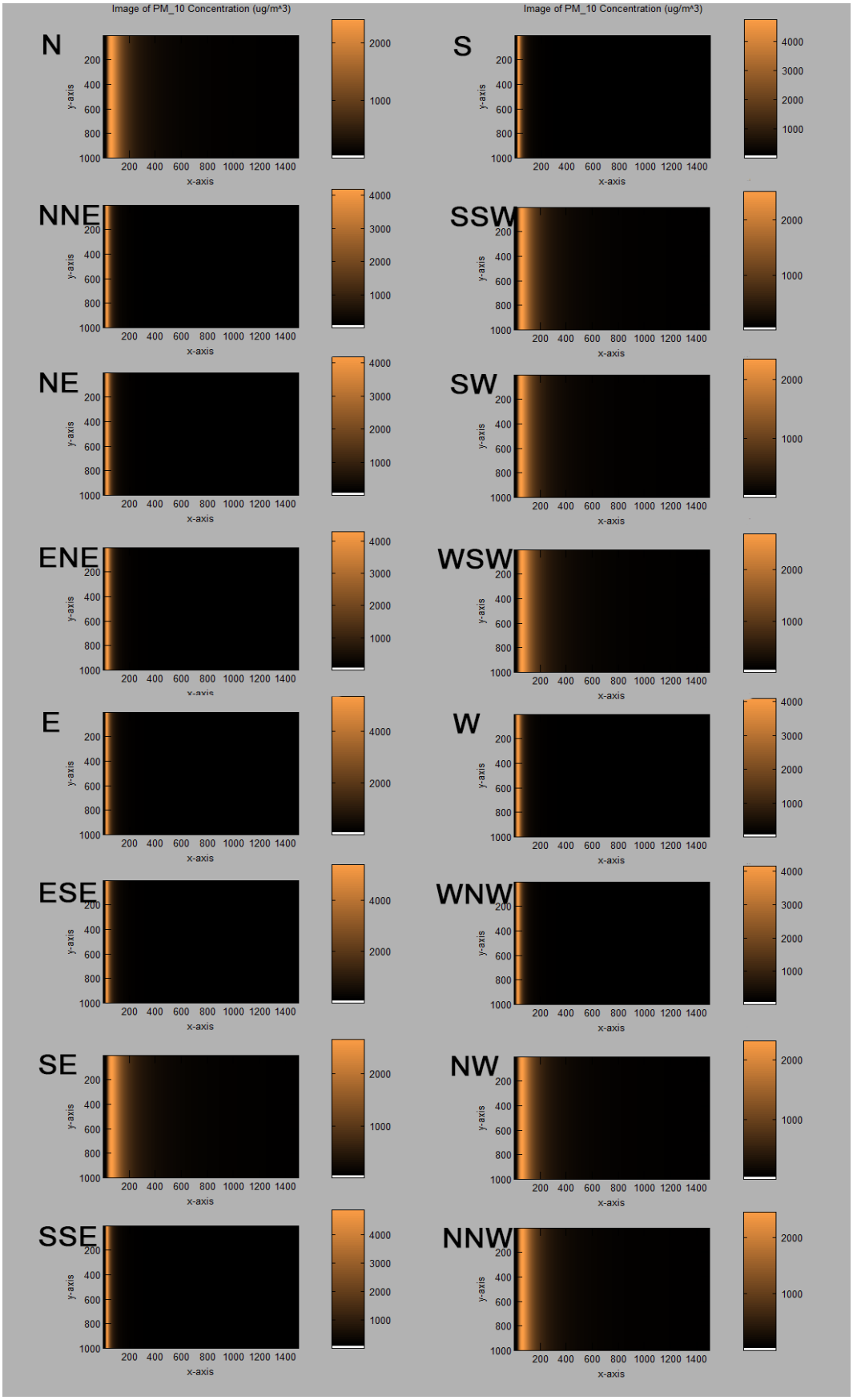

Figure 6. Dispersion profile of PM_{10} pollutants during summer with strong/moderate insolation

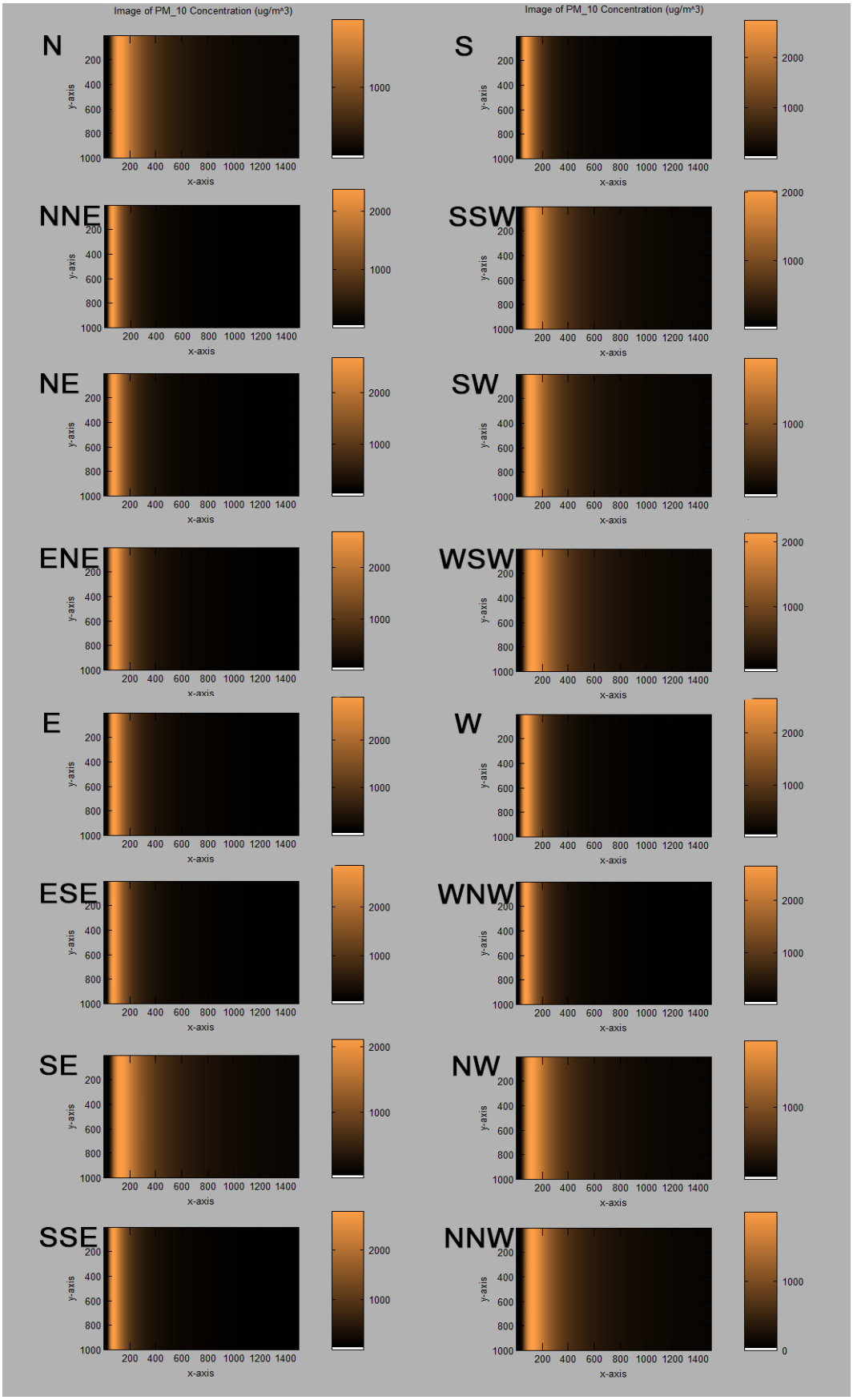

Figure 7. Dispersion profile of PM_{10} pollutants during summer with slight insolation

Table 4(a). Summary of dispersion profile of PM_{10} and NO_x pollutants at AEATPP during summer

Wind Direction	Strong/moderate insolation							
	PM_{10}				NO_x			
	Region Exceeding National Standard Limit (150 µg/m³) x (km)		Maximum value (µg/m³)	Location of maximum value x (km)	Region Exceeding National Standard Limit (100 µg/m³) x (km)		Maximum value (µg/m³)	Location of maximum value x (km)
	From	To			From	To		
N	0.48	8.44	2410.79	1.3	0.68	4.04	342.95	1.42
NNE	0.22	2.8	4181.91	0.62	0.3	1.7	618.61	0.66
NE	0.18	2.98	4185.66	0.64	0.28	1.8	626.25	0.7
ENE	0.18	3.2	4292.95	0.68	0.28	1.92	642.38	0.74
E	0.46	3.34	5358.88	0.58	0.52	2.02	766.25	0.58
ESE	0.46	3.32	5380.77	0.6	0.5	2	767.09	0.6
SE	0.62	9.58	2666.14	1.34	0.82	4.62	373.91	1.46
SSE	0.37	2.97	4870.39	0.62	0.43	1.79	698.2	0.66
S	0.37	2.87	4751.04	0.6	0.43	1.73	683.18	0.62
SSW	0.59	8.65	2516.96	1.24	0.77	4.15	356.43	1.32
SW	0.59	7.85	2348.71	1.12	0.77	3.77	335.7	1.18
WSW	0.66	9.6	2700.98	1.28	0.86	4.64	378.92	1.36
W	0.16	2.96	4091.52	0.64	0.26	1.78	617.68	0.7
WNW	0.2	2.9	4154.39	0.62	0.28	1.76	620.81	0.68
NW	0.42	8.14	2321.72	1.26	0.64	3.9	332.08	1.38
NNW	0.48	8.6	2450.89	1.32	0.7	4.12	347.86	1.44

Table 4(b). Summary of dispersion profile of PM_{10} and NO_x pollutants at AEATPP during summer

Wind Direction	Slight insolation							
	PM_{10}				NO_x			
	Region Exceeding National Standard Limit (150 µg/m^3) x (km)		Maximum value (µg/m^3)	Location of maximum value x (km)	Region Exceeding National Standard Limit (100 µg/m^3) x (km)		Maximum value (µg/m^3)	Location of maximum value x (km)
	From	To			From	To		
N	0.86	18.44	1965.53	2.48	1.32	7.86	275.68	2.74
NNE	0.42	8.42	2371.87	1.28	0.64	4.02	338.43	1.42
NE	0.46	11.08	2675.34	1.56	0.72	5.34	371.91	1.78
ENE	0.5	12.28	2702.85	1.72	0.78	5.92	371.86	1.96
E	0.8	12.42	2899.71	1.62	1.04	6.02	395.86	1.78
ESE	0.74	11.56	2865.91	1.54	0.96	5.6	394.14	1.68
SE	1.06	21.16	2114.44	2.66	1.5	9.08	292.26	2.94
SSE	0.61	10.83	2767.64	1.54	0.83	5.23	383.43	1.7
S	0.61	10.25	2727.48	1.46	0.81	4.95	379.91	1.6
SSW	0.99	18.89	2017.03	2.44	1.41	8.07	281.94	2.66
SW	0.99	16.91	1896.59	2.22	1.37	7.19	267.8	2.42
WSW	1.1	21.2	2130.46	2.58	1.54	9.1	294.39	2.84
W	0.44	11.08	2661.35	1.56	0.7	5.34	370.39	1.78
WNW	0.46	10.76	2660.23	1.52	0.72	5.18	370.85	1.72
NW	0.82	17.72	1912.48	2.4	1.26	7.54	269.42	2.66
NNW	0.9	18.84	1990.22	2.52	1.34	8.04	278.54	2.78

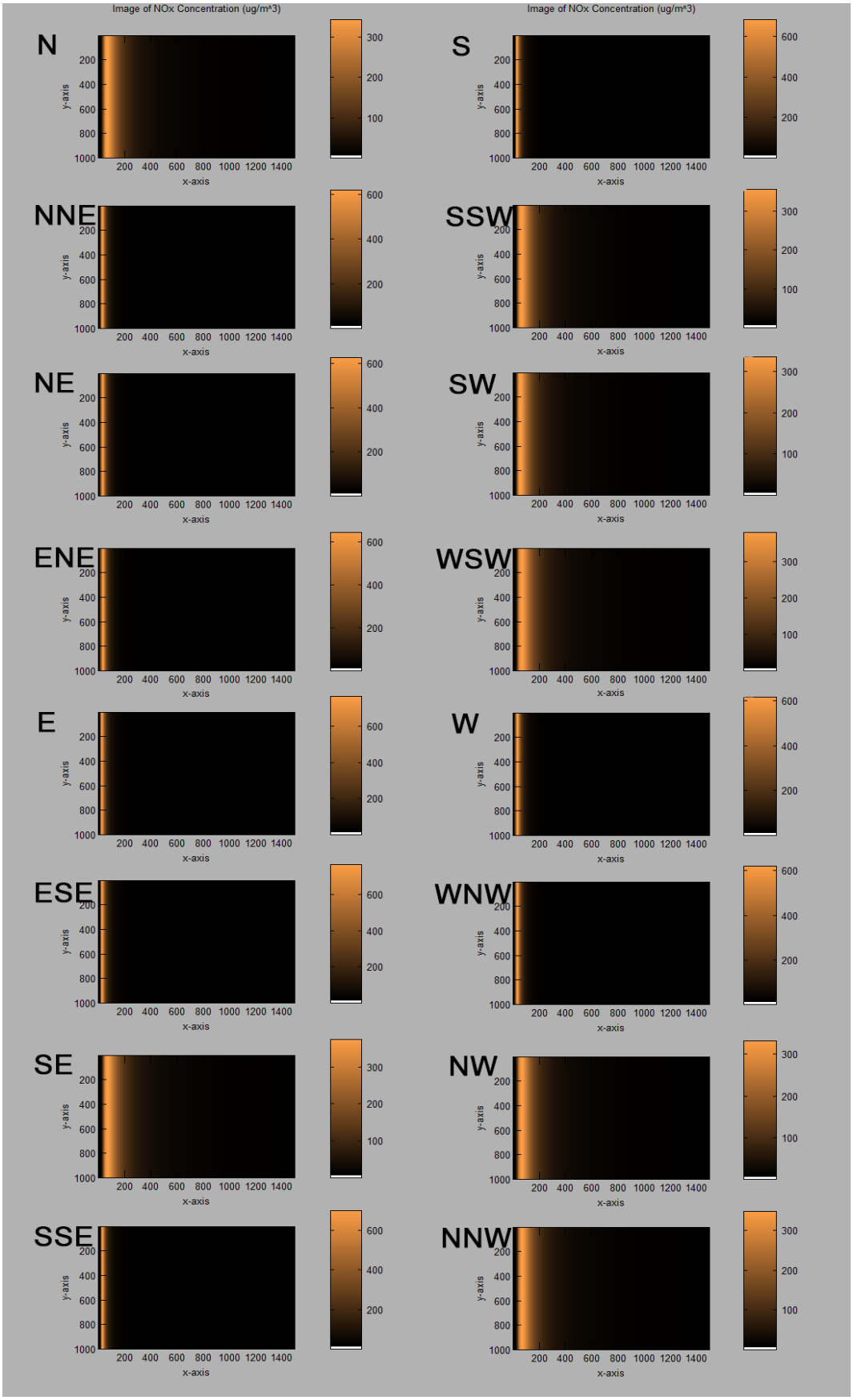

Figure 8. Dispersion profile of NO_x pollutants during summer with strong/moderate insolation

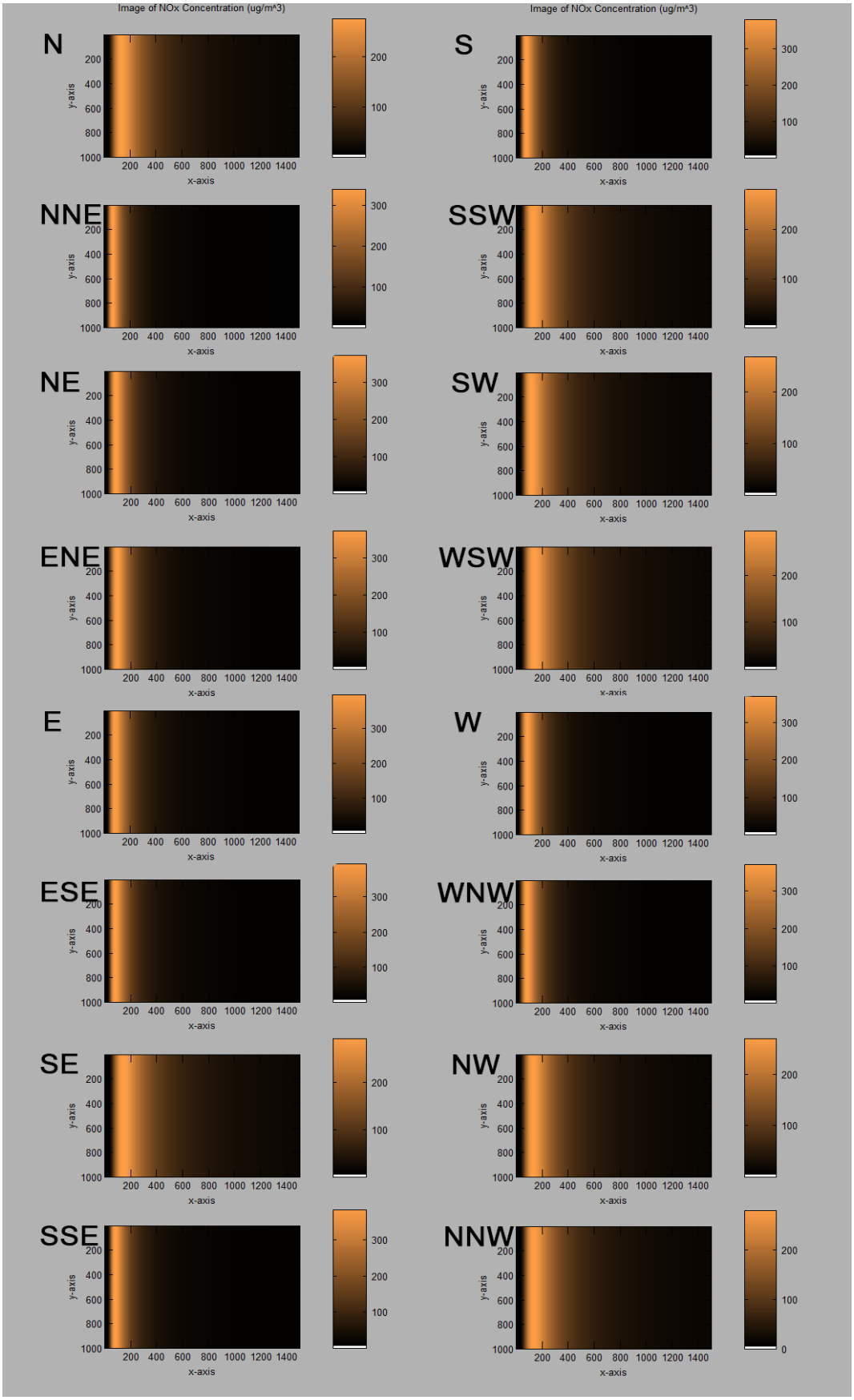

Figure 9. Dispersion profile of NO_x pollutants during summer with slight insolation

4. CONCLUSION

In this study, the dispersion of PM_{10} and NO_x from AE-ATPP plumes was successfully simulated using the Gaussian Plume Model in *Freemat*. The information on stacks and meteorological data at the site were among the input parameters in the simulation. Results have revealed that scenarios of greatest maximum ground concentration values are less dispersed and are located near the stacks. The dispersion varies with wind speed and temperature as manifested in the differences in results in January and July. During summer with strong/moderate insolation, PM_{10} with the highest maximum ground concentration values of 5380.77 $\mu g/m^3$ and NO_x with 767.09 $\mu g/m^3$ are both located at x = 0.60 km in the ESE scenario. Furthermore, regions where the concentrations of PM_{10} and NO_x exceed the Turkish government's national standard limit are present in all scenarios. This emphasizes the need for comprehensive environmental monitoring in areas proximal to AE-ATPP and mitigation strategies to lower the ground concentrations of these pollutants for the safety of populated areas nearby.

ACKNOWLEDGEMENT

There is no funding associated with the work featured in this article.

DECLARATION OF ETHICAL STANDARDS

The authors of this article declare that the materials and methods used in this study do not require ethical committee permission and/or legal-special permission.

AUTHORS' CONTRIBUTIONS

Yusof-den Jamasali: Design of study, modeling, simulation, article writing.

Şeref Turhan: Supervisor of Y. Jamasali, an expert in Environmental and Nuclear Physics, article writing and editing.

Aybaba Hançerlioğulları: An expert in Environmental and Nuclear Physics, writing and editing.

Aslı Kurnaz: An expert in Environmental and Nuclear Physics, writing and editing.

CONFLICT OF INTEREST

There is no conflict of interest in this study.

REFERENCES

[1] Manisalidis I., Stavropoulou E., Stavropoulos A., and Bezirtzoglou E., "Environmental and Health Impacts of Air Pollution: A Review", ***Front. Public Health***, 8: 14, (2020).

[2] Eze I. C. *et al.*, "Long-term air pollution exposure and diabetes in a population-based Swiss cohort", ***Environment International***, 70: 95–105, (2014).

[3] Shah A. S. V. *et al.*, "Short term exposure to air pollution and stroke: systematic review and meta-analysis", ***BMJ***, p. h1295, (2015).

[4] Mulder D., Ed., "Soil disinfestation", ***Developments in agricultural and managed-forest ecology***, no. 6. Amsterdam ; New York : New York: Elsevier Scientific Pub. Co. ; distributors for the U.S. and Canada, Elsevier North-Holland, (1979).

[5] Peirce J. J., Weiner R. F., Vesilind P. A., and Vesilind P. A., "Environmental pollution and control", ***4th ed. Boston: Butterworth-Heinemann***, (1998).

[6] Zhang C., Yao Q., and Sun J., "Characteristics of particulate matter from emissions of four typical coal-fired power plants in China", ***Fuel Processing Technology***, 86(7): 757–768, (2005).

[7] Kouprianov V. I., "Influence of lignite quality on airborne emissions from power generation in the Russian Far East and in Northern Thailand", ***Fuel Processing Technology***, 76(3): 187–199, doi: 10.1016/S0378-3820(02)00023-1, (2002).

[8] Nazari S., Shahhoseini O., Sohrabi-Kashani A., Davari S., Paydar R., and Delavar-Moghadam Z., "Experimental determination and analysis of CO_2, SO_2 and NO_x emission factors in Iran's thermal power plants", ***Energy***, 35(7): 2992–2998, doi: 10.1016/j.energy.2010.03.035, (2010).

[9] Basu S. and Debnath A. K., "Power Plant Instrumentation and Control Handbook: A Guide to Thermal Power Plants", ***Power Plant Instrumentation and Control Handbook***, *Elsevier*, i–ii. doi: 10.1016/B978-0-12-819504-8.09011-9, (2019).

[10] Athar M., Ali M., and Khan M. A., "Gaseous and particulate emissions from thermal power plants operating on different technologies", ***Environ Monit Assess***, 166(1–4): 625–639, doi: 10.1007/s10661-009-1028-0, (2010).

[11] Seinfeld J. H. and Pandis S. N., "Atmospheric chemistry and physics: from air pollution to climate change", ***2nd ed. New York: J. Wiley & Sons***, (2006).

[12] Cheng W.-L., Chen Y.-S., Zhang J., Lyons T. J., Pai J.-L., and Chang S.-H., "Comparison of the Revised Air Quality Index with the PSI and AQI indices", ***Science of The Total Environment***, 382(2–3): 191–198, doi: 10.1016/j.scitotenv.2007.04.036, (2007).

[13] Zhan D., Kwan M.-P., Zhang W., Yu X., Meng B., and Liu Q., "The driving factors of air quality index in China", ***Journal of Cleaner Production***, 197: 1342–1351, (2018).

[14] Mohan M. and Kandya A., "An Analysis of the Annual and Seasonal Trends of Air Quality Index of Delhi", ***Environ Monit Assess***, 131(1–3): 267–277, (2007).

[15] Sharma R. *et al.*, "Inferring air pollution from air quality index by different geographical areas: case study in India", ***Air Qual Atmos Health***, 12(11): 1347–1357, (2019).

[16] Din S. A. M., Yahya N. N.-H. N., and Abdullah A., "Fine Particulates Matter ($PM_{2.5}$) from Coal-fired Power Plant in Manjung and its Health Impacts", ***Procedia - Social and Behavioral Sciences***, 85: 92–99, (2013).

[17] Van Den Elshout S., Léger K., and Nussio F., "Comparing urban air quality in Europe in real time", ***Environment International***, 34(5): 720–726, 2008).

[18] Büke T. and Köne A., "Assessing Air Quality in Türkiye: A Proposed, Air Quality Index", ***Sustainability***, 8(1): 73, (2016).

[19] Ma Z. *et al.*, "Characteristics of NO_x emission from Chinese coal-fired power plants equipped with new technologies", ***Atmospheric Environment***, 131: 164–170, (2016).

[20] Lazaridis M., "First Principles of Meteorology and Air Pollution", ***Environmental Pollution***, 19, Dordrecht: Springer Netherlands, (2011).

[21] Ainslie B. and Jackson P. L., "The use of an atmospheric dispersion model to determine influence regions in the Prince George, B.C. airshed from the burning of open wood waste piles", ***Journal of Environmental Management***, 90(8): 2393–2401, (2009).

[22] Nihalani S. A., Mishra Y., and Juremalani J., "Emission Control Technologies for Thermal Power Plants", ***IOP Conf. Ser.: Mater. Sci. Eng.***, 330: 012122, (2018).

[23] Kaygusuz K., "Energy Use and Air Pollution Issues in Türkiye", ***CLEAN Soil Air Water***, 35(6): 539–547, (2007).

[24] Myllyvirta L., Farrow A., Anhäuser A., "Future Air Quality and Health Impacts of the planned Afşin A power plant expansion", ***Centre for Research on Energy and Clean Air***. https://energyandcleanair.org/wp/wp-content/uploads/2022/04/Afsin-expansion_-Report.pdf, (2022).

[25] Güvenç U., Bakir H., and Duman S., "Investigation the Success of Semidefinite Programming for the Estimating of Fuel Cost Curves in Thermal Power Plants", ***Politeknik Dergisi***, 24(1): 247–254, (2021).

[26] Ersoy Ö., Özbay M., Karafaki F. Ç., and Erol D., "The Environmental Importance of Flue Gas Purification Systems; Case of Yatağan Thermal Power Station", ***Journal of Polytechnic***, 20(3): 570-577, (2017).

[27] Tontu M., "Kömür Yakıtlı Termik Santralin Çalışma Esnekliğinin İncelenmesi", ***Politeknik Dergisi***, 24(3): 893–902, (2021).

[28] Şirin M., "How many thermal power plants are there in Türkiye? Names of all thermal power plants!", ***Haberler***, https://www.haberler.com/haberler/turkiye-de-kac-tane-termik-santral-var-tum-14307220-haberi/ (2023).

[29] Peavy H. S., Rowe D. R., and Tchobanoglous G., "Environmental Engineering", ***McGraw-Hill series in water resources and environmental engineering. New York: McGraw-Hill***, (1985).

[30] Ministry of Environment, "Air quality protection regulation (AQPR)", ***Official Gazette 19269, Ankara MOE***, (1986).

[31] European Environment Agency, "World Health Organization (WHO) air quality guidelines (AQGs) and estimated reference levels (RLs)". https://www.eea.europa.eu/publications/status-of-air-quality-in-Europe-2022/europes-air-quality-status-2022/world-health-organization-who-air (2024).